Updates on the Hotspot and the Perseus-Pisces supercluster Excess Observed by the Telescope Array Experiment

Jihyun Kim[1*], *Dmitri* Ivanov[1], *Kazumasa* Kawata[2], *Hiroyuki* Sagawa[2], and *Gordon* Thomson[1] for the Telescope Array Collaboration

[1]High Energy Astrophysics Institute and Department of Physics and Astronomy, University of Utah, Salt Lake City, Utah 84112-0830, USA
[2]Institute for Cosmic Ray Research, University of Tokyo, Kashiwa, Chiba 277-8582, Japan

Abstract. The Telescope Array (TA) experiment, the largest observatory studying ultra-high energy cosmic rays in the northern hemisphere, has reported evidence for two medium-scale anisotropies. The first, known as the TA hotspot, is an excess in the arrival direction distribution for events with energies greater than 5.7×10^{19} eV. More recently, an additional excess of events with energies greater than $10^{19.4}$ eV appearing in the direction of the Perseus-Pisces supercluster has been named the PPSC excess. In this presentation, we will update the status of the TA hotspot and the PPSC excess results using the most recent data measured by the TA surface detector array.

1 Introduction

Ultra-high-energy cosmic rays (UHECRs) are energetic charged particles originating from outer space that impinge on Earth's atmosphere with energies above 10^{18} eV. There have been many efforts to elucidate their origin; however, it is still challenging since cosmic magnetic fields are ubiquitous in the universe and bend UHECR trajectories from their sources. However, for higher energy cosmic rays having $E > 10^{19.5}$ eV, they have still reasonable deflections to search for their sources by studying their arrival direction distribution.

Anisotropy studies reveal patterns in the arrival direction distribution that may be indicative of UHECR's source locations. In 2014, the Telescope Array (TA) experiment reported anisotropy in the arrival direction distribution of UHECR events with energy greater than 57 EeV (1 EeV = 10^{18} eV), called the TA hotspot [1]. By using 5 years of data collected by the TA surface detector array, we found an excess of events in the Ursa Major constellation, using an oversampling analysis with an intermediate angular scale of 20°. Using the Li-Ma analysis method, the maximum significance of excess compared to the isotropic background was calculated to be 5.1σ at the position of (146.7°, 43.2°) in equatorial coordinates. The global significance of this excess was estimated to be 3.4σ by Monte Carlo simulations. A number of sources have been suggested, including M82, Mrk 180 [2], Mrk 421 [3], and filaments of galaxies connected to the Virgo cluster [4]. However, it is necessary to get higher statistics to discern the nature of the TA hotspot.

Recently, TA observed an additional excess of events with energy greater than $10^{19.4}$ eV. While investigating the energy spectrum mismatch between TA and Pierre Auger Observatory, we found excesses in the energy spectrum in energy bins of $10^{19.4}$ eV, $10^{19.5}$ eV, and $10^{19.6}$ eV. We examined their arrival direction distributions to understand what causes these excesses in the energy spectrum and found the new excess of events appearing in the direction of the Perseus-Pisces supercluster (PPSC), which has been named the PPSC excess [5, 6].

Here, we update the TA hotspot and the PPSC excess using the most up-to-date data measured by the TA surface detector array.

2 Telescope Array Experiment

The TA experiment is the largest UHECR observatory in the northern hemisphere. It is located at 39.3° N 112.9° W in the west desert of Utah, USA. Its elevation is 1400 m above sea level, which is perfectly suitable for observing the maximum development of air showers. TA is a hybrid experiment, using a combination of ground array and air-fluorescence techniques. A total of 507 surface detectors (SDs) are deployed with 1.2 km spacing over an area of approximately 700 km^2. Each SD counter consists of two-layers of plastic scintillator to sample the footprint of the air shower when it reaches Earth's surface [7]. Three fluorescence detector (FD) stations overlook the SD array using 38 fluorescence telescopes viewing 3°–31° in elevation. The FDs measure the ultra-violet light generated as the shower passes through the gas of the atmosphere [8].

3 Description of the Dataset

In this analysis, we use data measured by the TA SD array that has the highest statistical power. The data acquisition

*e-mail: jihyun@cosmic.utah.edu

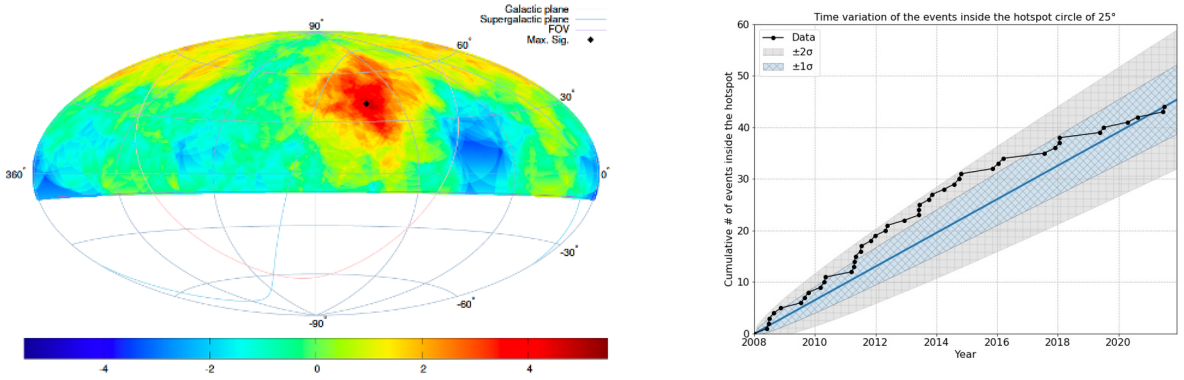

Figure 1. The sky map of the TA hotspot and the increase rate of events inside the hotspot circle. (Left) It is shown that the Li-Ma significance using a 25°-circle angular window in equatorial coordinates for 14 years of SD events with energies greater than 57 EeV. The black diamond indicates the maximum Li-Ma significance position at (144.0°, 40.5°). The color code indicates an excess (red) and a deficit (blue) of events compared to isotropy. **(Right)** The black dots represent the cumulative number of events inside the hotspot circle of 25° from the most significant excess to the isotropy at (144.0°, 40.5°). The blue solid line indicates the estimated event rate inside the hotspot. The light blue and gray bands show $\pm1\sigma$ and $\pm2\sigma$ deviations from the linear increase rate.

period is between May 11, 2008, and May 10, 2022. The selection criteria employed in this analysis are as follows:
1. Each event must include at least five SD counters.
2. The reconstructed primary zenith angle must be less than 55°.
3. Both the geometry and lateral distribution fits must have χ^2/degree of freedom value less than 4.
4. The angular uncertainty estimated by the geometry fit must be less than 5°.
5. The fractional uncertainty in S800 estimated by the lateral distribution fit must be less than 25%.
6. The largest signal counter surrounded by four working counters, there must be one working counter to the left, right, down, up on the grid of the largest signal counter, but they do not have to be immediate neighbors of the largest signal counter.

The reconstructed SD energy is normalized to the FD calorimetric energy using hybrid events [9]. For the hotspot analysis, we adopt the same energy threshold and selection criteria that were used in the original hotspot paper [1]. The energy threshold is 57 EeV and the selection criteria are looser than those described above to include more events at higher energies while keeping reasonable energy and angular resolutions. For the PPSC excess analysis, the energy threshold is set to $10^{19.4}$ eV, where an excess in the energy spectrum was observed. The total number of events used for the hotspot analysis is 205 and the energy and angular resolutions of the events are 10% and 1.0°, respectively. On the other hand, the total number of events used for the PPSC excess analysis is 1060, and energy and angular resolutions of the events are 20% and 1.5°, respectively [10].

4 Methods and Results

We conduct oversampling searches to investigate intermediate scale anisotropies in the data sets. Oversampling calculations are done at grid points in equatorial coordinates, having 0.1° steps in right ascension (0°–360°) and declination (−10°–90°). Specifically, at each grid point, we sum over the number of events in a given angular scale circle for the data, defined as $N_{\rm on}$. ($N_{\rm off} = N_{\rm tot} - N_{\rm on}$) Then, we generate 10^5 events assuming an isotropic flux taking into account the geometrical exposure $g(\theta) = \sin\theta\cos\theta$ as a function of zenith angle (θ) because the detection efficiency for this energy range is ∼100% regardless of zenith angle θ. Using these isotropic background events, we sum over the number of events in the given angular scale circle in the same manner we did for the data, which defines $\alpha = N_{\rm iso,on}/N_{\rm iso,off}$ for exposure ratio of *on* to *off*. Then, by comparing the oversampling of observed data to the isotropic background events, the statistical significance of the excess of events at each grid point is calculated by the following equation [11]:

$$S_{\rm LM} = \sqrt{2}\left[N_{\rm on}\ln\left(\frac{(1+\alpha)N_{\rm on}}{\alpha(N_{\rm on}+N_{\rm off})}\right) + N_{\rm off}\ln\left(\frac{(1+\alpha)N_{\rm off}}{N_{\rm on}+N_{\rm off}}\right)\right]^{1/2}. \quad (1)$$

4.1 TA Hotspot

In 14 years of TA SD data, we take 205 events with energies greater than 57 EeV and then examine their arrival direction distribution using the Li-Ma method with 25° oversampling angular size, which gave the maximum excess of events in the previous analysis using 12 years of data [5]. The most significant excess to the isotropy was found at (144.0°, 40.5°) in equatorial coordinates. Inside the 25°-circle from the position, 44 out of 205 events are detected, whereas only 16.9 events are expected from the isotropic distribution. The Li-Ma significance is calculated to be 5.1σ. The left panel of Figure 1 shows the sky map with the Li-Ma significance indicating excess (red) and deficit (blue) of events compared to the isotropic sky. The black diamond represents the maximum Li-Ma significance position. We estimate how often such excess could appear

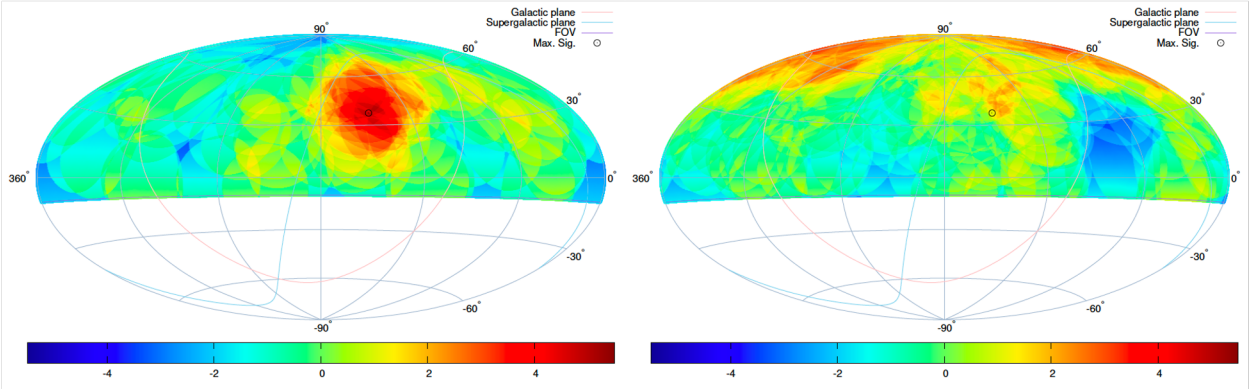

Figure 2. The sky map of the TA hotspot for independent data sets. It is shown that the Li-Ma significance using a 25°-circle angular window in equatorial coordinates for first 5-year events and the last 9-year events with energies greater than 57 EeV. The open circles indicate the maximum Li-Ma significance position at (144.0°, 40.5°) obtained from the 14-year data. **(Left)** For the first 5-year events, which is the period the TA hotspot was observed for the first time, the local maximum Li-Ma significance is calculated to be 5.0σ. **(Right)** For the last 9-year events, the local maximum Li-Ma significance is calculated to be 2.5σ, which still indicates an excess of events in the hotspot direction.

anywhere in TA's field of view by Monte Carlo simulation. The chance probability is estimated to be 7.4×10^{-4}, corresponding to $\sim 3.2\sigma$.

In addition, we examine the time variation of the hotspot by counting the cumulative number of events inside the hotspot as a function of time. The result is shown on the right panel of Figure 1. Inside the 25°-circle from the maximum excess position of (144.0°, 40.5°), the cumulative number of observed events is shown with $\pm 1\sigma$ and $\pm 2\sigma$ bands deviations from a linear increase rate. We conclude that the increase rate of the events inside the hotspot circle is consistent with a constant within 2σ fluctuation.

We also investigate the excess of events by dividing the whole data set into two periods for independent analysis: the first 5 years and the last 9 years. We split data into the first 5 years and the remaining because the first 5-year data was the one we found the hotspot in 2014 [1]. Figure 2 shows the sky maps of independent analysis. In the first 5-year data, 22 out of 72 events are observed inside the 25°-circle from the maximum excess position of (144.0°, 40.5°), taken from the 14-year result, whereas 5.2 events are expected from the isotropy. The local maximum Li-Ma significance is calculated to be 5.0σ. In the last 9-year data, 22 out of 133 events are detected inside the oversampling circle while 11.6 events are expected. The local maximum Li-Ma significance is calculated to be 2.5σ, which still indicates an excess of events in the hotspot direction.

4.2 Perseus-Pisces Supercluster Excess

Here, we revisit the PPSC excess using 14 years of TA SD data. By adopting the same methodology used for the original hotspot study [1], we conduct the oversampling analysis with 20°-radius angular windows. The data selection criteria are described in Section 3, which are tighter than those for the hotspot analysis since we have more events at lower energies and need to maintain good energy and angular resolution.

In 14 years of TA SD data, we have 1060, 685, and 413 events with energy greater than $10^{19.4}$ eV, $10^{19.5}$ eV, and $10^{19.6}$ eV, respectively. The oversampling analysis results are summarized as follows: the Li-Ma significances are calculated to be 3.8σ at (17.4°, 36.0°), 3.8σ at (19.0°, 35.1°), and 3.5σ at (19.7°, 34.6°) for $E \geq 10^{19.4}$ eV, $E \geq 10^{19.5}$ eV, and $E \geq 10^{19.6}$ eV, respectively. The sky maps of the PPSC excess for each energy threshold are shown in Figure 3. We observe consistent excesses of events in the direction of the PPSC.

We examine whether another excess of events is observed close to other nearby supercluster locations. We choose all the similar major structures to the PPSC in TA's field of view within 150 Mpc, which is the GZK horizon assuming proton primaries: Virgo cluster (17 Mpc), PPSC (70 Mpc), Coma supercluster (90 Mpc), Leo supercluster (135 Mpc), and Hercules supercluster (135 Mpc). Figure 3 (d) shows their center locations overlaid with the excess map. The data do not show an excess at any of the locations of other nearby major structures other than the PPSC. None of them have Li-Ma significances greater than 1σ. The PPSC is a unique and significant structure in TA's field of view because it is the closest supercluster other than the Local supercluster where we reside and its location is next to the Local Void [12, 13], where the magnetic field strength is presumed to be weaker than other structures in the cosmic web.

It is suggestive that the excess in the data falls in the direction of the PPSC. We estimate how often this happens by chance. First, we generate many Monte Carlo event sets, each containing the same number of events as the data. We throw Monte Carlo events isotropically according to the acceptance of the TA SD. We conduct the same oversampling analysis for each Monte Carlo event set using the Li-Ma method. After that, we count as successes the number of sets where the point of maximum

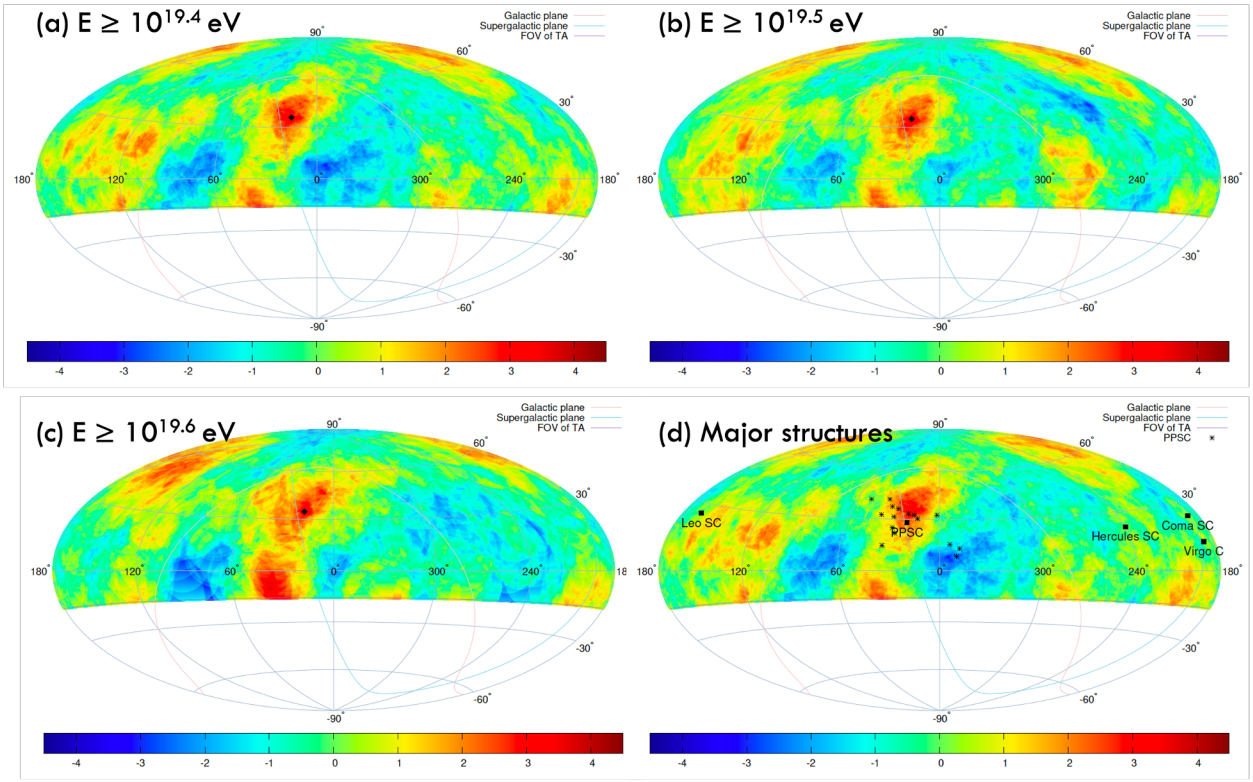

Figure 3. The sky maps of the PPSC excess using Hammer projection. It is shown that the Li-Ma significance using a 20°-circle angular window in the equatorial coordinates for different energy thresholds: (a) $E \geq 10^{19.4}$ eV, (b) $E \geq 10^{19.5}$ eV, and (c) $E \geq 10^{19.6}$ eV. In addition, (d) shows the nearby major large-scale structures with the Li-Ma significance map with $E \geq 10^{19.4}$ eV. The color code indicates an excess (red) and a deficit (blue) of events compared to isotropy at each grid point.

Li-Ma significance is at least as significant as in the data, and also occurs at least as close to the PPSC as in the data: ($S_{\rm mc} \geq S_{\rm obs}$) and ($\theta_{\rm mc} \leq \theta_{\rm obs}$). Finally, we calculate the chance probability of having equal or higher excess as close to the PPSC as in the data. We obtain for 3.1σ, 3.2σ, and 3.0σ for $E \geq 10^{19.4}$ eV, $E \geq 10^{19.5}$ eV, and $E \geq 10^{19.6}$ eV, respectively. We also perform the same calculations for the chance probability of having equal or higher excess as close to any of the nearby major structures we discussed above as PPSC. The results are 2.5σ, 2.6σ, and 2.4σ for $E \geq 10^{19.4}$ eV, $E \geq 10^{19.5}$ eV, and $E \geq 10^{19.6}$ eV, respectively. We conclude that the results indicate that a cosmic ray source may exist in the direction of the PPSC.

5 Summary

In this work, intermediate scale anisotropy studies were conducted using 14 years of TA SD data. We have persistent evidence for the TA hotspot at the highest energies, $E > 57$ eV. The global significance of such excess appearing by chance anywhere in TA's field of view is estimated to be 3.2σ. The new excess in slightly lower energy events having $E \geq 10^{19.4}$ eV in the direction of the Perseus-Pisces supercluster has been identified. The chance probability of having an excess as close to the Perseus-Pisces supercluster as the data is estimated to be 3.2σ.

References

[1] Abbasi, R.U., *et al.*, Astrophysical Journal Letters, **790**, L21 (2014).
[2] He, H.-N., *et al.*, Physical Review D, **93**, 043011 (2016).
[3] Fang, K., Fujii, T., Linden, T., and Olinto, A.V., Astrophysical Journal **794**, 126 (2014).
[4] Kim, J., Ryu, D., Kang, H., Kim, S., and Rey, S.-C., Science Advances **5** eaau8227, (2019).
[5] Kim, J., Ivanov, D, Kawata, K., Sagawa, H., and Thomson, G., PoS(ICRC2021)328 (2021)
[6] Abbasi, R.U., *et al.*, https://arxiv.org/abs/2110.14827 (2021)
[7] Abu-Zayyad, T., *et al.*, Nuclear Instruments Methods in Physics Research Section a-Accelerators Spectrometers Detectors and Associated Equipment, **689**, 87 (2012).
[8] Tokuno, H., *et al.*, Nuclear Instruments Methods in Physics Research Section a-Accelerators Spectrometers Detectors and Associated Equipment, **676** 54 (2012).
[9] Abu-Zayyad, T., *et al.*, Astrophysical Journal Letters, **768**, L1 (2013).
[10] Abbasi, R.U., *et al.*, Astrophysical Journal, **862**, 91 (2018).

[11] Li, T.-P. and Y.-Q. Ma, Astrophysical Journal Letters, **272**, 317 (1983).
[12] Courtois, H.M., et al., Astronomical Journal, **146**, 69 (2013).
[13] Tully, R.B., *et al.*, Astrophysical Journal, **880**, 24 (2019).